Transition Metal Chemistry (2007) 32:117–124
DOI 10.1007/s11243-006-0132-z

Synthesis, characterization, theoretical calculations and catalase-like activity of mixed ligand complexes derived from alanine and 2-acetylpyridine

Nasser Mohammed Hosny*
Chemistry Department, Faculty of Education, Suez-Canal University, 42111 Port-Said, Egypt

Received 3 August 2006; accepted 21 September 2006

Abstract

Mixed ligand complexes $[M(2\text{-AP})(Ala)Cl_x \cdot mH_2O]nH_2O$, where (M = Co^{II}, Ni^{II}, Cr^{III} and Fe^{III}, 2-AP = 2-acetylpyridine, Ala = alanine, x = 2–3, m = 0–1 and n = 3–5] are synthesized and characterized by elemental analysis, FTIR, UV/Vis., MS, TG, measurements and semi-empirical calculations ZINDO/1 and PM3. The results suggest an octahedral geometry for all isolated complexes. FTIR spectra show that alanine coordinates to the metal ions as a neutral unidentate through the amino nitrogen where 2-acetylpyridine coordinates to the metal ion in a bidentate manner through carbonyl oxygen and pyridyl nitrogen. Semi-empirical calculations have been used to study the molecular geometry and the harmonic vibrational spectra with the purpose to assist the experimental assignment of the complexes. The Fe complex showed significant activity as a catalase-like model.

Introduction

Chemistry of metal complexes derived from amino acids has developed because of possible biological interest [1]. Most of the studies concerned with the synthesis and properties of these complexes and the factors influencing their stereoselective formation, but more recent studies [2–4] emphasized the reactivity of coordinated alanine in the hope of finding simple and easily interpretable models of reactivity of some biological systems which contain metals. Many classes of enzymes either contain metals or need a metal ion as a cofactor. Grosser has shown that l-alanine exerts antioxidant action [5]. Tumour cells are sensitive to the effects of iron chelators because of the critical requirement for Fe in proteins that play essential roles in DNA synthesis (*e.g.*, ribonucleotide reductase) and energy production (*e.g.*, cytochromes) [6]. The incorporation of cobalt into the coenzyme is quite surprising because it is the least abundant first row 3d transition metal in the earth's crust and in sea water. Therefore, a very special functionality is to be expected. For a long time, nickel has been the only element of the late 3d transition metals for which a biological role could not be definitely established [7]. According to recent knowledge [8] nickel is present in four different kinds of enzymes, in different oxidation states; in urease enzymes of bacteria and plants contain five or six coordinated nickel(II) bound to N,O-ligands, Ni–Fe hydrogenase, CO-dehydrogenase, acetyl-CoA synthase and F-430 [7]. Acetylpyridine amino acids complexes may serve as models for pyridoxylidene–amino acids systems which are considered to be intermediates in biologically important amination processes [9]. Metal complexes derived from glycine, 3-acetylpyridine with metal acetates and chlorides have been described. It was found that in case of metal chlorides the lower pH (2–4) block NH_2 as NH_3^+, glycine and 3-acetylpyridine coordinate separately to metal ion to form mixed ligand complexes, and the condensation between the amino group of glycine and carbonyl group of 2-acetylpyridine does not occur [10].

The area of gas phase transition metal ion chemistry has experienced explosive growth in the recent past [11]. Rapid advances in computer hardware and theoretical methodology have established the computation of structures and molecular properties of organic compounds as a complementary tool for experimentalists. For transition metal complexes and bioinorganic systems the exploitation of modeling as a powerful and reliable tool has only just started. This is due to inherent complications, first from partially filled d-orbitals and second to the size of biological molecules [12]. Quantum mechanical approaches [13] empirical force field calculations [14] or empirical correlations [15] may be appropriate to predict and/or interpret molecular structures and properties.

Hydrogen peroxide is a byproduct of aerobic respiration; nevertheless in the presence of reductive metals [Fe^{II} or Cu^{I}], it can be converted to hydroxyl radicals whose deleterious effects on cell components is well documented [16, 17]. Therefore all living cells have devised a sophisticated machinery to suppress or at least control H_2O_2 production. The catalase enzymes which are able to disproportionate H_2O_2 into less

* Author for correspondence: E-mail: nasserh56@yahoo.com

harmful dioxygen and water are an important part of this machinery. The enzyme catalase catalyzes the rapid decomposition of hydrogen peroxide by the following reaction:

$$2H_2O_2 \longrightarrow 2H_2O + O_2 \text{ (gas)}$$

Several studies have been carried out on Mn complexes to act as catalase-like [18, 19]. In this paper, the synthesis, thermal, magnetic and spectral data of Co^{II}, Ni^{II}, Cr^{III} and Fe^{III} complexes with alanine and 2-acetylpyridine have been described. Also, the geometrical parameters using semi-empirical calculations ZINDO/1 and PM3 have been determined. To validate our methodology a comparison of the experimental IR frequencies of the complexes under investigation with the computed values has been used. The catalytic mechanism of Fe^{III} complex is discussed.

Experimental

Reagents

All the chemicals used were of analytical grade and were used without further purification.

Measurements

Carbon and hydrogen contents were determined at the micro analytical unit of Cairo University. Molar conductance measurements of the complexes (10^{-3} M) in DMSO were carried out with a conductivity bridge YSI model 32. Infrared spectra were measured using KBr discs and a Nujol mull on a Mattson 5000 FTIR spectrometer. Calibration with the frequency reading was made with polystyrene film at Mansoura University. Electronic spectra were recorded on a UV2 Unicam UV/vis spectrometer using 1 cm stoppered silica cells. Thermal analysis measurements (t.g.a., d.t.a.) were recorded on a Schimadzu model 50 instrument using 20 mg samples. The nitrogen flow rate and heating were 20 cm^3 min^{-1} and 10 °C min^{-1}, respectively. Mass spectra of the solid complex were recorded on Joel TMS-DX 303 (EI-GC 245) mass spectrometer at Cairo University.

Preparation of metal complexes

A general procedure was followed for all the complexes. An aqueous solution of alanine (0.01 mol) in 10 cm^3 H_2O was added to 0.01 mol of 2-acetyl pyridine in 10 cm^3 MeOH. The metal chlorides was dissolved in a minimum amount of H_2O (5 cm^3), then added to the reaction mixture of the ligand dropwise with constant stirring, and finally heated under reflux for 3 h on a hot plate at 50 °C. The mixture was evaporated until dry. The residual was dissolved in an excess of MeOH followed by drops of Et_2O to precipitate the solid complex. The isolated metal complexes were filtered-off, washed with H_2O, MeOH, recrystallized from dichloroethane and preserved in a vacuum desiccator over anhydrous calcium chloride.

Catalytic activity of the metal complexes

The metal complex was mixed with H_2O_2 (0.01–0.1 N) in a 5 cm^3 stoppered flask for 2 h. The metal complex catalyzed the decomposition of H_2O_2 and O_2 was evolved. After 2 h the reaction was arrested by 20 cm^3 2 N H_2SO_4 and titrated with 0.1 N $KMnO_4$ solution. The difference in titre values of the $KMnO_4$ solution before and after the catalyzed decomposition was followed. The experiment was similarly conducted with the various metal complexes. The catalytic decomposition of H_2O_2 was studied at various H_2O_2 concentrations and complex concentrations [20].

Computational details

Molecular geometries of all forms of complexes were optimized by molecular mechanics and the semi-empirical ZINDO/1 and PM3 methods using the hyperchem series of programs [21]. Molecular mechanics technique was used to investigate rapidly the geometries of the suggested structures. The low lying conformers obtained from this search were then optimized at ZINDO/1 and PM3 (Polak-Ribiere) RMS 0.01 kcal. Where applicable, these methods are commonly used for the calculations of energy states of transition metal complexes.

Results and discussion

The analytical data for the complexes, together with physical properties are shown in Table 1.

The results indicate that the complexes are hygroscopic and soluble in water or DMSO but insoluble in most common organic solvents. The chloride test assured coordination for chloride counter ions. The complexes react with $AgNO_3$ in HNO_3 solution, this fact is taken as evidence that chloride ions are bonded to the metal in the complexes. Also, low molar conductivity values in DMSO (1.9–2.0 Ω^{-1} cm^2 mol^{-1}) suggest that the complexes are non-electrolytes [22] and support the aforementioned fact. The presence of IR bands assigned to carbonyl group of 2-acetylpyridine and amine group of alanine indicate that these ligands bind separately to the metal ions to form mixed ligand complexes and the Schiff bases resulting from the condensation of these two groups does not form. This behavior has been attributed to lowering of the pH of the metal chloride complexes [10]. The lower pH value supports the Zwitter ion character of alanine. Under these conditions the nucleophilic attack from the lone pair of electrons on the amine nitrogen to the carbonyl carbon of the ketone will be difficult. The presence of a protonated OH group in the alanine

Table 1. Analytical data and physical properties of the complexes

Compound	Color	M.P (°C)	Found (Calcd.) (%)				Λ^a in DMSO
			C	H	M	Cl	
$[Co(2\text{-}AP)(Ala)Cl_2H_2O]3H_2O$	Green	200	28.6 (29.1)	4.8 (5.3)	14.7 (14.1)	17.0 (17.2)	2.0
$[Ni(2\text{-}AP)(Ala)Cl_2H_2O]5H_2O$	Green	245	26.7(26.8)	5.4 (5.8)	15.4 (15.0)	16.2 (15.9)	1.9
$[Cr(2\text{-}AP)(Ala)Cl_3]5H_2O$	Green	> 300	25.5 (25.6)	4.9 (5.1)	12.2 (11.9)	22.0 (22.7)	1.9
$[Fe(2\text{-}AP)(Ala)Cl_3]4H_2O$	Brown	125	26.7 (27.1)	4.6 (4.8)	12.7 (13.1)	24.5(24.0)	2.0

[a] Ω^{-1} cm^2 mol^{-1}.

has been confirmed by an acidity test. The presence of water molecules inside and outside the coordination sphere has been determined from thermal analyses (TGA) measurements.

FTIR

The most important IR assignments of the complexes have been determined by careful comparison of the spectra of complexes with the spectra of alanine and 2-acetylpyridine. The spectra of complexes show broad band starting from 2700 to 3600 cm^{-1} under which the bands assigned to ν(OH) of alanine, coordinated water and $\nu(NH_2)$ exist. Also, the spectra of the complexes show a strong band in the case of Fe^{III}) complex and shoulder bands in the case of other complexes at 1742 cm^{-1} assigned to $\nu(C=O)$ of protonated and uncoordinated carboxyl group of amino acid [23]. The spectra of the complexes show bands at *ca.* 1649 cm^{-1} assignable to $\delta(NH_2)$. Also, the spectra of all complexes show bands in the region 3400–3446 cm^{-1} assigned to ν(OH) of carboxyl group of alanine. The vibrations which can be affected due to the coordination of 2-acetylpyridine are $\nu(C=O)$, $\nu(C=C)$ and $\nu(C=N)$ bands observed between 1698 and 1443 cm^{-1}, ring breathing modes near 995 cm^{-1} an out-of-plane C–H deformation band at 780 cm^{-1} skeletal mode at 740 cm^{-1} and an out-of-plane C–C deformation band around 410 cm^{-1}in the spectrum of 2-acetylpyridine. The spectra of the complexes show bands at ~1660 cm^{-1} assigned to $\nu(C=O)$py, the ring breathing mode at 1000 cm^{-1} and ring skeletal mode at 700 cm^{-1}. Also, the spectra of the complexes show bands in the 1598–1607 cm^{-1} region assignable to $\nu(C=N)$ and 1418–1422 cm^{-1} assignable to $\nu(C=C)$ [24]. In addition, bands in the 1023–1038 cm^{-1} region are assigned to ρ_w (NH_2).

In the far IR region (650–200 cm^{-1}), the bands appearing at 630, 590 and 420 cm^{-1} may be assigned to $\rho_r(NH_2)$ and$(C=O)$ and C–C out-of-plane deformation mode, respectively [24]. Several new bands appearing in this region of spectra at 540, 380 and ≈300 cm^{-1} are assigned to ν(M–N), ν(M–O) and ν(M–Cl), respectively [25].

Comparison of IR spectra of the free ligands and their metal complexes show that 2-acetylpyridine coordinates Co^{II}, Ni^{II}, Cr^{III} and Fe^{III} in a neutral bidentate fashion through the carbonyl oxygen and the pyridyl nitrogen. This behavior is supported by the following evidence: (i) The shift of the band at 1698 cm^{-1} assigned to carbonyl oxygen to a lower wave number ~1660 cm^{-1}. (ii) The shift of the band assigned to $\nu(C=N_{py})$ at 1587 cm^{-1} to higher wave number ~1590 cm^{-1}. (iii) The presence of new bands in the 520–540 and 330–380 cm^{-1} regions assigned to ν(M–N) and ν(M–O), respectively.

At the same time alanine can coordinate to Co^{II}, Ni^{II}, Cr^{III} and Fe^{III} as protonated monodentate through the amino nitrogen. This suggestion is supported by the following evidence: (i) The presence of a band at 1742 cm^{-1} assigned to carbonyl group of protonated and uncoordinated carboxyl group of alanine [23]. (ii) The shift of the band at 1623 in the free ligand assigned to $\delta_s NH_2$ to higher wave number ≈1649 cm^{-1} indicating the participation of this group in the coordination.

The experimental and theoretically calculated frequencies by semi-empirical calculations ZINDO/1 and PM3 methods are listed in Table 2. The cause of the difference between the calculated and observed frequencies may result from the hydrogen bonded water molecules which have not been taken into consideration in the optimized molecules. Also, the experimental data were obtained from solid state, whereas the calculated harmonic frequencies are for the gas phase.

Electronic spectra and magnetic moments

The electronic spectrum of $[Co(2\text{-}AP)(Ala)Cl_2H_2O]$ $3H_2O$ in DMSO shows two bands at 14,815 and 16,667 cm^{-1} assigned to $^4T_{1g} \rightarrow {}^4A_{2g}(\nu_2)$ and $^4T_{1g} \rightarrow {}^4T_{1g}(P)(\nu_3)$ transitions, respectively. The observation of these two bands suggests an octahedral geometry around cobalt(II) ion [26]. The spectrum shows a band at 22,007 cm^{-1} assigned to $L \rightarrow M$ charge transfer. Also, the ligand field parameters [B = 714, β = 0.74 and 10 Dq = 7860 cm^{-1}. where B = Racah parameters; β is the nephelauxetic parameter $\beta = B(\text{complex})/B(\text{free ion})$] fall in the range suggested for octahedral geometry. The value of the magnetic moment 5.1 B.M. suggests the existence of octahedral geometry around Co^{II} ion (Figure 1).

The electronic spectrum of $[Ni(2\text{-}AP)(Ala)Cl_2H_2O]$ $5H_2O$ in DMSO shows three bands at 10,395, 14,700 (splitted), and 23,310 cm^{-1} assigned respectively to $^3A_{2g} \rightarrow {}^3T_{2g}(\nu_1)$, $^3A_{2g} \rightarrow {}^3T_{1g}(\nu_2)$ and $^3A_{2g} \rightarrow {}^3T_{1g}(P)$

Table 2. Observed and calculated wave numbers (cm^{-1}) of $[Co(2\text{-}AP)(Ala)Cl_2H_2O]3H_2O$, $[Ni(2\text{-}AP)(Ala)Cl_2H_2O]5H_2O$, $[Cr(2\text{-}AP)(Ala)Cl_3]5H_2O$ by ZINDO/1 and $[Fe(2\text{-}AP)(Ala)Cl_3]4H_2O$ by PM3 semi-empirical calculations

Co complex (Exp.)	Co complex (Calcd)	Ni complex (Exp.)	Ni complex (Calcd)	Fe complex (Exp.)	Fe complex (Calcd)	Cr complex (Exp.)	Cr complex (Calcd)	Assignment
1742	1713	1742	1709	1743	1713	1743	–	$\nu(C=O)_{Ala}$
1655	1676	1654	1672	1655	1686	1659	1665	$\nu(C=O)_{Py}$
1624	1622	1649	1609	1634	–	1619	1624	$\delta_s(NH_2)$
1607	1581	1598	1583	1600	1560	1590	1584	$\nu(C=N)$
1485	1469	1500	1534	1496	1494	1495	1476	$\nu(C=C)$
1418	1421	1422	1422	1385	1388	1439	1440	ν(C–O)
1377	1351	1371	1351	1350	1354	1357	1332	ν(C–N)
1023	1023	1038	1049	1030	1032	1041	1049	$\delta_d(NH_2)$
1000	968	990	968	990	1006	945	932	Ring breathing mode
785	792	788	807	770	797	855	833	Out-of-plane CH
630	627	627	640	643	654	655	640	$\rho_w(NH_2)$
584	579	590	586	575	590	605	606	π (C=O)
542	558	541	553	510	502	532	528	ν(M–N)
423	435	408	382	429	420	364	385	C–C out-of-plane
380	390	365	354	336	335	360	–	ν(M–O)
323	327	290	295	290	296	330	343	ν(M–Cl)

ν, stretching; δ, in-plane deformation; γ, out-of-plane deformation; w, wagging; ρ, rocking.

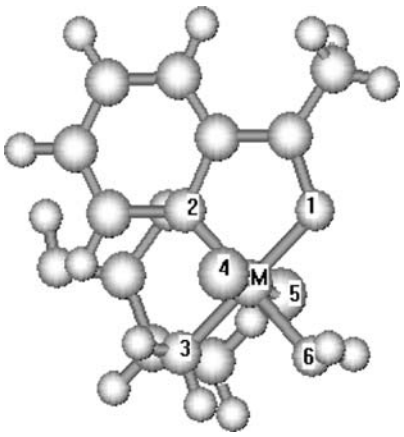

Fig. 1. $M = Co^{II}$ or Ni^{II}.

(ν_3) in octahedral geometry around Ni^{II} ion the splitting of the band at 14,700 cm^{-1} resulted from spin-orbital coupling [26]. Also, the ligand field parameters (B = 775, β = 0.74 and 10 Dq = 8500 cm^{-1}) fall in the range suggested for octahedral geometry of Ni^{II}. The magnetic moment value 3.3 B.M. gives additional evidence for octahedral geometry around Ni^{II} ion (Figure 1).

The electronic spectrum of $[Cr(2\text{-}AP)(Ala)Cl_3]5H_2O$ in DMSO shows two bands at 16,260 and 23,310 cm^{-1} assigned to $^4A_{2g} \rightarrow {}^4T_{1g}$ and $^4A_{2g} \rightarrow {}^4T_{1g}$(F) transitions, respectively. Also, the spectrum shows a shoulder band at 15,105 cm^{-1} assigned to a forbidden transition. The presence of these bands suggests an octahedral geometry around Cr^{III} ion [26]. The magnetic moment value (3.9 B.M.) suggests the presence of three unpaired electrons [27] (Figure 2).

The electronic spectrum of $[Fe(2\text{-}AP)(Ala)Cl_3]4H_2O$ (Figure 2) in DMSO shows two bands. The first observed at 19,607 cm^{-1} assigned to d–d transitions where the second at 25,189 cm^{-1} assigned to L $\rightarrow$ M charge transfer transition. The value of magnetic moment (5.8 B.M.) is very close to the spin only value expected for high spin Fe^{III}.

Thermal analyses

The thermal analyses (T.G and D.T.G) curves of the complexes were carried out within a temperature range from room temperature up to 800 °C. The estimated mass losses were computed based on the TG results and the calculated mass losses were computed using the results of microanalyses (Table 3). The determined temperature range, percent losses in mass and thermal effects accompanying the changes in the solid complex on heating are given in Table 3.

Table 3 relates the following findings. The Co^{II} complex gives four stages of decomposition pattern. It is noticed that the hydrated water has two types; the first type within the temperature range 65–150 °C, represents the loss of one water molecule of hydration (estimated mass loss 3.4%, theoretical 4.4%). The second type (155–315 °C) represents the loss of three water molecules c [28] with an estimated mass loss of 14.6%, theoretical 13.2%. The activation energy of

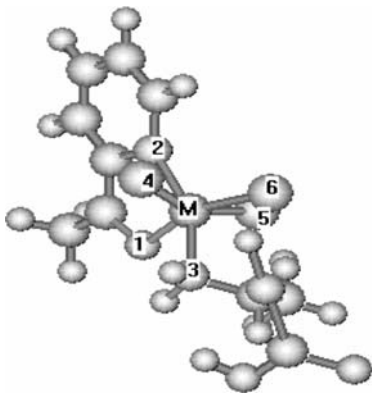

Fig. 2. $M = Cr^{III}$ or Fe^{III}.

Table 3. Thermoanalytical results (TG) of Co^{II}, Ni^{II}, Cr^{III} and Fe^{III} metal complexes

Complex	*T* range (°C)	Mass loss Estim (Calcd.%)	Assignment
$[Co(2\text{-AP})(Ala)Cl_2H_2O]3H_2O$	65–150	3.40 (4.4)	Loss of H_2O molecule of hydration
	155–315	14.6 (13.2)	Loss of $3H_2O$ hydrogen bonded-coordinated
	315–431	16.2 (17.6)	Loss of Cl_2 molecule
	431–719	35.9 (36.4)	Loss of alanine and CH_3O
$[Ni(2\text{-AP})(Ala)Cl_2H_2O]5H_2O$	48–180	11.5 (12.1)	Loss of $3H_2O$ molecules of hydration
	185–292	11.5 (12.1)	Loss of $3H_2O$ hydrogen bonded-coordinated
	293–416	16.6 (15.0)	Loss of Cl_2 molecule
	418–787	30.1 (29.2)	Loss of alanine and CH_3O
$[Cr(2\text{-AP})(Ala)Cl_3]5H_2O$	54–176	8.0 (7.9)	Loss of $2H_2O$ molecules of hydration
	178–292	11.8 (10.2)	Loss of $3H_2O$ molecules hydrogen bonded
	294–460	24.5 (23.2)	Loss of 3Cl
	462–702	18.1 (19.0)	Loss of alanine molecule
	702–757	4.0 (3.3)	Loss of CH_3
	759–995	18.7 (17.3)	Loss of Pyridyl
$[Fe(2\text{-AP})(Ala)Cl_3]4H_2O$	39–139	6.2 (6.2)	Loss of $2H_2O$ molecules of hydration
	139–225	7.6 (8.3)	Loss of $2H_2O$ molecules hydrogen bonded
	226–485	24.5 (25.2)	Loss of 3Cl
	487–750	38.3 (38.2)	Loss of alanine and Pyridyl

this step is 84.7 KJ mol^{-1}. The third stage of decomposition within the temperature range 315–431 °C represents the loss of Cl_2 molecule (estimated mass loss 16.2%, theoretical 17.6%) with activation energy 90.9 KJ mol^{-1}. The last decomposition step within the temperature range 431–619 °C with an estimated mass loss 35.9%, theoretical 36.4% with activation energy 133 KJ mol^{-1} is ascribed to loss of alanine molecule and acetyl group, leaving a CoPy residue.

The thermogram of Ni^{II} complex shows that at 48–180 °C, three water molecules of hydration are lost (estimated mass loss 11.57%, theoretical 12.1%). The second step (185–292 °C) involves the loss of three water molecules; two of them are hydrogen bonded and they are not coordinating to the metal ion and one coordinates to the metal ion [28] (estimated mass loss 11.52%, theoretical 12.1%). The activation energy of this step is 132.5 KJ mol^{-1}. The last step within the temperature range (418–787 °C) represents the loss of an alanine molecule and the acetyl moiety (estimated mass loss 30.1%, theoretical 29.2%). The activation energy of this step is 101.1 KJ mol^{-1}.

Thermal analyses curves (TG and DTG) of [Cr (2-AP)(Ala)Cl_3]$5H_2O$ shows that this complex decomposes in six steps. The first step (54–176 °C) corresponds to the loss of two molecules of water of hydration (estimated mass loss 11.8%, theoretical 10.2%). The second step (178–292 °C) corresponds to the loss of three molecules of water hydrogen bonded [28] (estimated mass loss 8.0%, theoretical 7.9%). The third step (294–460 °C) corresponds to the loss of three chloride ions (estimated mass loss 24.5%, theoretical 23.2%).The activation energy of this step is 109.14 KJ mol^{-1}. The fourth step in the temperature range 462–702 °C represents the loss of alanine (estimated mass loss 18.0%, theoretical 19.0%). Then, the methyl group is lost in the temperature range 702–757 °C (the estimated mass loss 4.0%, theoretical 3.3%) the last step corresponds to the loss of pyridyl moiety (estimated mass loss 18.7%, theoretical 17.3%).

$[Fe(2\text{-AP})(Ala)Cl_3]4H_2O$ decomposes in four stages the first stage from 39 to 134 °C corresponds to the loss of two molecules of water of hydration (estimated mass loss 6.2%: theoretical 6.2%). The second stage (135–225 °C) represents the loss of two water molecules hydrogen bonded [28] (estimated mass loss 7.6%; theoretical 8.3%) with activation energy 90.18 KJ mol^{-1}. The third step in the temperature range (226–485 °C) represents the loss of 3Cl in two successive steps (estimated mass loss 25.2%, theoretical 24.5%). The last step (487–750 °C) represents the loss of alanine and pyridyl moieties (estimated mass loss 38.3%, theoretical 38.2%) . The activation energy of this step 92.86 KJ mol^{-1}.

The kinetic parameters such as activation energy ΔE were evaluated graphically by employing the Coats–Redfern relation [29]:

$$\log[\log\{W_f/(W_f - W)\}/T^2] = \log[AR/\theta E(1 - (2RT/E))] - E/2.303RT$$

where W_f is the mass loss at the completion of the reaction, W the mass loss up to temperature T, R the gas constant, E the activation energy in KJ mol^{-1}, θ is the heating rate and $1-(2RT/E)\approx 1$. A plot of the left-hand side of the above equation against $1/T$ gives a slope from which E was calculated. In general, the stages of decomposition of the complexes can be written as shown below.

$$[M(2-AP)(Ala)Cl_x \cdot mH_2O]nH_2O \xrightarrow{39-180\,^\circ C} [M(2-AP)(Ala)Cl_x \cdot mH_2O] + nH_2O$$

$$[M(2-AP)(Ala)Cl_x \cdot mH_2O] \xrightarrow{140-290\,^\circ C} [M(2-AP)(Ala)Cl_x] + mH_2O$$

$$[M(2-AP)(Ala)Cl_x] \xrightarrow{294-450\,^{\circ}C} [M(2-AP)(Ala)] + Cl_x$$

$$[M(2-AP)(Ala)] \xrightarrow{420-750\,^{\circ}C} [M(2-AP)] + (Ala)$$

where x = 2–3; m = 0–1; n = 3–5. The above Equation represents a general scheme for thermal decomposition of mixed ligand complexes.

Mass spectra

The mass spectrum of Fe^{III} complex (Figure 3) shows the molecular weight corresponding to the suggested formula after loss of water and two molecules of hydrogen. The fragmentation pattern of Fe^{III} complex is represented as follows.

$$\underset{m/z\ 256\ (7.6\%)}{[Fe(Ala)CCOCl_2]} \xleftarrow{-Py,HCl,H} [Fe(2\text{-}AP)(Ala)Cl_3]$$

$$\xrightarrow{H_2,Cl,2-AP} \underset{m/z\ 214\ (8.0\%)}{[FeAlaCl_2]}$$

$$[Fe(Ala)CCOCl_2] \xrightarrow{-Cl_2} \underset{m/z\ 185\ (8.5\%)}{[Fe(Ala)CCO]}$$

$$\xrightarrow{-CCO} \underset{m/z\ 146\ (100\%)}{[FeNH_2CH_2CH_2COOH]^{+\cdot}}$$

$$[Fe\text{-}NH_2-CH_2-CH_2COOH]^{+\cdot} \xrightarrow{-NH_3} \underset{m/z\ 129\ (17.5\%)}{[Fe(CHCH_2COOH)]^{+\cdot}}$$

$$[Fe(CHCH_2COOH)]^{+\cdot} \xrightarrow{-CH_3COOH} \underset{m/z\ 69\ (20\%)}{FeC^{\cdot}}$$

The above Equation represents the fragmentation pattern of $[Fe(2\text{-}AP)(Ala)Cl_3]4H_2O$.

Structural parameters

The optimized structures of Co^{II}, Ni^{II}, Cr^{III} and Fe^{III} complexes are visualized in (Figures 1, 2) and selected parameters of their structural data are summarized in Table 4.

The ligand 2-acetylpyridine can coordinate to Co^{II}, Ni^{II}, Cr^{III} and Fe^{III} in a bidentate fashion through carbonyl oxygen and pyridyl nitrogen. The distance between the Co atom and the carbonyl oxygen O1–Co is 0.03 Å longer than the average O–Co bonds (1.959 Å) in the corresponding crystal structure [30]. This may be explained by the depletion of charge on oxygen atom because of the flow of electrons from the adjacent ring system. While in case of Ni^{II}, Fe^{III} complex the distance between the Ni atom and the carbonyl oxygen O1–Ni and the distance between O1-Fe are 0.068 Å shorter than the average O–Ni bonds (1.984 Å) and O–Fe bonds (2.071 Å) in corresponding structures [30, 31] because of strong electrostatic attraction between the bonding oxygen and these cations. The distance between cobalt, chromium and pyridyl nitrogen N2–Co is (0.073 Å) and N2–Cr is (0.040 Å) shorter than the average values of N–Co and N-Cr in corresponding complexes indicating the strong electrostatic attraction between the pyridyl nitrogen and these ions [30, 31]. Also, the N2–Ni bond is shorter than N–Ni average distance in experimentally determined structures for the same reason. On the other hand, alanine can coordinate Co^{II} or Ni^{II} (Figure 1) in a mondentate fashion through the amino nitrogen.

The distances between N3–Co and N3–Ni are shorter by (0.029 and 0.09 Å), respectively, than the average value of corresponding crystal structures [30] indicating the strong electrostatic attraction between the amino group nitrogen and the cations.

Catalytic activity

The elucidation of the detailed mechanism of enzyme action is a problem of common interest to the physico- and bio-scientists. The difficulty of this problem seems to be due to lack of the detailed structure of the enzyme molecules and the role played by the metal ions in the metalloenzymes. This important problem of

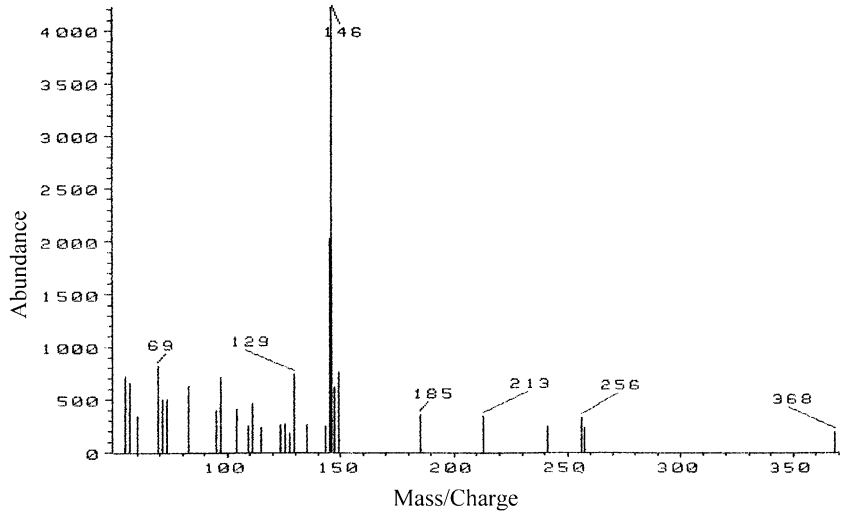

Fig. 3. MS spectrum of $Fe(2\text{-}AP)(Ala)Cl_3]4H_2O$.

Table 4. Selected structural parameters of the optimized complexes, bond distance (Å) and bond angles in (°) as obtained from ZINDO/1 method

Distance between atoms (Å)	M = Co	M = Ni	M = Cr	M = Fe[a]
M–O1	1.99	1.916	2.11	1.87
M–N2	2.06	1.99	2.13	1.88
M–N3	2.09	2.037	2.15	1.92
M–Cl4	2.45	2.38	2.37	2.26
M–Cl5	3.53	3.49	2.89	2.25
M–O6	2.1	2.02	–	–
M–Cl6	–	–	2.37	2.26
Angle (°)				
Cl4–M–Cl5	123	122.8	159.6	166.8
O6–M–N2	99.95	98.2	–	–
Cl6–M–N2	–	–	76.8	92.2
N3–M–N2	97	94.9	169.3	166.6
O6–M–Cl5	51	52.1	–	–
Cl6–M–Cl5	–	–	98.6	95.8
N2–M–Cl4	171.7	170.5	94.5	84.9
O1–C–C–N2	81.7	84.89	76.8	89.3
N3–C–C–C	62.04	59.72	110.6	91.3

[a]As obtained from PM3 method.

enzyme action may be approached by constructing and studying small model molecules with enzyme-like activity.

The catalytic mechanism

The detailed mechanism of the catalytic action of $[Fe(2\text{-}AP)(Ala)Cl_3]4H_2O$ for the decomposition of hydrogen peroxide is illustrated in Scheme 1.

The activity (K) of the complex to disproportionate H_2O_2 was measured as a function of the complex and the substrate concentration. The relation between the activity (K) calculated as first order rate constant and different concentrations of the catalyst at constant concentration of H_2O_2 is given in Table 5.

Table 5. Activity of Fe complex at constant concentration of H_2O_2 (0.018 mol l^{-1}) at 25 °C

Conc. of the complex (mol l^{-1})	Activity (K s^{-1})
2.26×10^{-3}	2.1×10^{-5}
4.50×10^{-3}	1.8×10^{-4}
6.8×10^{-3}	2.4×10^{-4}
9.0×10^{-3}	3.2×10^{-4}

Metal ion specificity

A rather extensive study was carried out on the catalase-like activity of chelates formed by 2-AP and Ala with various metal ions. The metal ions selected for this study include Cu^{II}, Co^{II}, Ni^{II}, Zn^{II} and Cr^{III}. Only 2-AP and Ala chelates of Fe^{III} showed remarkable catalytic activity for the decomposition of H_2O_2. The catalytic activity of 2-Ap, Ala chelates of all other metal ions listed above are negligible as compared to $[Fe(2\text{-}AP)(Ala)Cl_3]4H_2O$. Neither the size nor the charge of the metal ion can be the cause of this specificity, since some of the above ions have size and charge similar to Fe^{III}. It seems likely that this specificity is due to some special requirement on the detailed electronic structure of the metal ion [31–33]. In the present model catalyst the distribution of the electrons around the metal nucleus must be such as to make compound like I, II and III in Scheme 1 to have appropriate amounts of stability. While compound III is a highly unstable reaction intermediate (high activa-

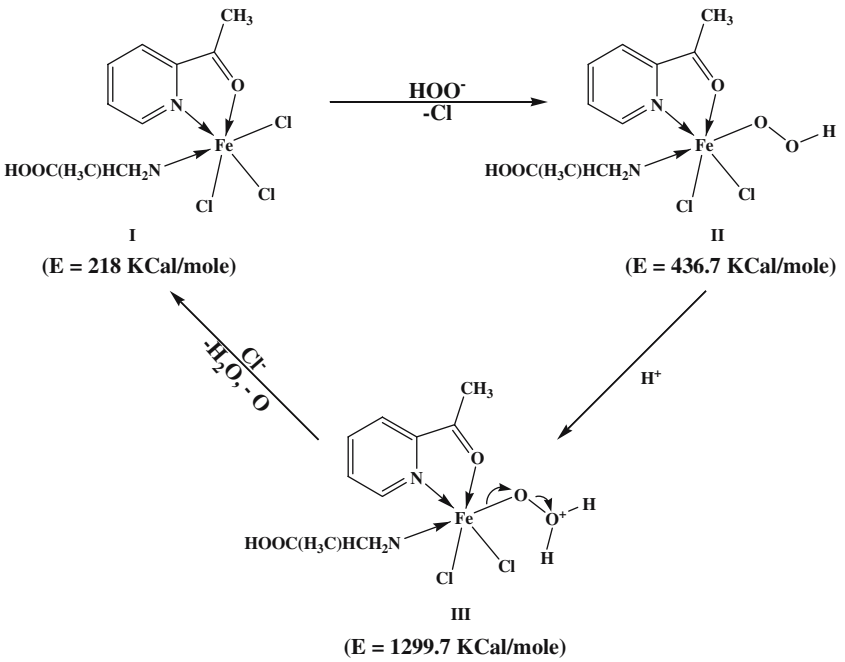

Scheme 1. The detailed mechanism of catalytic action of $[Fe(2\text{-}AP)(Ala)Cl_3]4H_2O$.

tion energy), since extremely stable reaction intermediate will prevent rapid regeneration of the original catalyst. It is suggested that one molecule of ^{-}OOH is combined to the complex, then it is protonated and decomposed to yield atomic oxygen and one molecule of water as indicated by Scheme 1. It is interesting to notice that compound I is potentially capable of combining with two ^{-}OOH ions to form [Fe(2-AP)(Ala)-$Cl(OOH)_2$] by replacing two of Cl^{-} by two ^{-}OOH, the decomposition of these two molecules will yield oxygen gas, two molecules of water and regenerate the catalyst.

For the decomposition of H_2O_2. The energy calculated using molecular mechaniques method.

References

1. A. Pasini and L.J. Casella, *Inorg. Nucl. Chem.*, **36**, 2133 (1979).
2. C.R. Bhattacharjee and P.K. Choudhury, *Transition Met. Chem.*, **26**, 730 (2001).
3. L. Wang, J. Cai, Z.W. Mao, X.L. Feng and J.W. Huang, *Transition Met. Chem.*, **29**, 411 (2004).
4. M.M. Shoukry, E.M. Khairy and A.A. El-Sherif, *Transition Met. Chem.*, **27**, 656 (2002).
5. N. Grosser, S. Oberle, G. Berndt, K. Erdmannk and A. Hemmerle, *Biochem. Biophys. Res. Commun.*, **314**, 351 (2004).
6. D.E. Metzler, *J. Am. Chem. Soc.*, **79**, 485 (1957).
7. W. Kaim and B. Schwederski, *Bioinorganic Chemistry: Inorganic Elements in the Chemistry of Life, an Introduction and Guide*, John Wiley & Sons, 1994.
8. R. Cammack, *Adv. Inorg. Chem. Radiochem.*, **32**, 297 (1988).
9. D.E. Metzler, *J. Am. Chem. Soc.*, **79**, 485 (1957).
10. N.A. Nawar, A.M. Shallaby, N.M. Hosny and M.M. Mostafa, *Transition Met. Chem.*, **26**, 180 (2001).
11. T. Shoeib, C.F. Rodriquez, K.W.M. Siu and A.C. Hopkinson, *Phys. Chem. Chem. Phys.*, **3**, 853 (2001).
12. P. Comba and R. Remenyi, *Coord. Chem. Rev.*, **9**, 238 (2003).
13. A. R. Leach, *Molecular Modeling*, Longman Edinburgh,1996.
14. A.K. Rappe and C.J. Casewit, *Molecular Mechanics across Chemistry*, University Science Books, Sausalito, 1997.
15. J. Zupan and J. Gasteiger, *Neural Networks for Chemists: an Introduction*, VCH Verlag, New York, Weinheim, 1993.
16. E. Stadtman, P. Berlett and P. Chock, *Proc. Natl. Acad. Sci. U.S.A.*, **87**, 384 (1990).
17. B. Halliwell and J. Gutteridge, *Methods in Enzymology*, Academic Press, San Diego, 1990.
18. V. Daier, H. Biava, C. Palopoki, S. Shova, J. Tuchagues and S. Signorella, *J. Inorg. Biochem*, **98**, 1806 (2004).
19. J. Gao and S.H. Zhong, *J. Mol. Cat. A: Chem.*, **186**, 25 (2000).
20. L. Jose and V.N.R. Pillai, *Polymer*, **39**, 231 (1998).
21. Hyperchem 7, developed by Hypercube Inc. 2002.
22. W.J. Geary, *Coord. Chem. Rev.*, **7**, 81 (1971).
23. K. Nakamoto, *Infrared Spectra of Inorganic and Coordination Compounds*, John Wiley, New York, 1970.
24. S.K. Sahni, S.K. Sangal, S.P. Gupta and V.B. Rana, *J. Inorg. Nucl. Chem.*, **39**, 1098 (1977).
25. J.R. Ferraro, *Low Frequency Vibrations of Inorganic and Coordination Compounds*, Plenum press, New York, 1971.
26. A.B.P. Lever, *Inorganic Electronic Spectroscopy*, Elsevier, Amsterdam, 1986.
27. F.A. Cotton and G. Wilkinson, *Advanced Inorganic Chemistry* (*A Comprehensive Text*), 4th edit., John Wiley, New York, 1980.
28. S. Cakir, E. Coskun, P. Naumov and E. Bicer, *J. Mol. Struc.*, **608**, 101 (2001).
29. A.W. Coats and J.P. Redfern, *Nature*, **20**, 68 (1964).
30. D. Kong, J. Reibenspies, A. Clearfield and A.E. Martell, *Inorg. Chem. Commun.*, **7**, 195 (2004).
31. W.H. Chen, H.H. Wei, G.H. Lee and Y. Wang, *Polyhedron*, **20**, 515 (2001).
32. A.G. Raso, J.J. Fiol, B. Adrover, P. Tauler, A. Pons, I. Mata, E.E. Spinosa and E. Molins, *Polyhedron*, **22**, 3255 (2003).
33. J. Gao, A.E. Martell and J.H. Reibenspies, *J. Inorg. Chim. Acta*, **346**, 23 (2003).